View metadata, citation and similar papers at core.ac.uk

brought to you by CORE

provided by DigitalCommons@University of Nebraska

University of Nebraska - Lincoln

DigitalCommons@University of Nebraska - Lincoln

Faculty Publications, Department of Physics and Astronomy

Research Papers in Physics and Astronomy

July 2003

Static and dynamic dipole polarizability of the helium atom using wave functions involving logarithmic terms

Mauro Masili
Centro Universitário Central Paulista, UNICEP, São Paulo, Brazil

Anthony F. Starace
University of Nebraska-Lincoln, astarace1@unl.edu

Follow this and additional works at: https://digitalcommons.unl.edu/physicsfacpub

 Part of the Physics Commons

Masili, Mauro and Starace, Anthony F., "Static and dynamic dipole polarizability of the helium atom using wave functions involving logarithmic terms" (2003). *Faculty Publications, Department of Physics and Astronomy*. 47.
https://digitalcommons.unl.edu/physicsfacpub/47

This Article is brought to you for free and open access by the Research Papers in Physics and Astronomy at DigitalCommons@University of Nebraska - Lincoln. It has been accepted for inclusion in Faculty Publications, Department of Physics and Astronomy by an authorized administrator of DigitalCommons@University of Nebraska - Lincoln.

Static and dynamic dipole polarizability of the helium atom using wave functions involving logarithmic terms

Mauro Masili
Centro Universitário Central Paulista, UNICEP, Rua Miguel Petroni 5111, 13 563-470 São Carlos, São Paulo, Brazil

Anthony F. Starace
Department of Physics and Astronomy, The University of Nebraska, 116 Brace Laboratory, Lincoln, Nebraska 68588-0111, USA
(Received 10 June 2002; revised manuscript received 15 May 2003; published 23 July 2003)

We present a calculation of the static and dynamic dipole polarizability of the helium atom using a variationally stable treatment that incorporates the coupled-channel hyperspherical representation of the wave functions. Inclusion of logarithmic terms in intermediate functions as well as the effect of an optimization procedure for the variational parameter are analyzed. When available, our coupled-channel results are compared with other values in the literature.

DOI: 10.1103/PhysRevA.68.012508 PACS number(s): 32.10.Dk, 32.80.−t

I. INTRODUCTION

It was demonstrated long ago that the wave function for the helium atom at the triple-collision point should formally be described as a power series in R and $\ln R$, where R is the hyperspherical radius [1,2]. However, this description has only been applied in calculations of energy levels [3–7]. The main effect of this expansion is to speed up the convergence of the calculated energy, reducing the large number of basis functions needed in usual variational calculations. More recent works [8–14] have demonstrated that alternative kinds of expansions, not involving logarithmic terms, can achieve benchmark energy levels with reasonable basis sizes. These methods involve double [9,11] and triple [12] basis sets, noninteger [8] or complex [13,14] powers of the expansion variables, or special kinds of configuration interaction expansions [10]. In a recent work, Popov and Ancarani [15] showed, in a rigorous mathematical study of the bound states of the helium atom, how the logarithmic terms, as suggested by Bartlett [1], are linked to the electron-electron interaction in the region of small radii. Nevertheless, they discussed only briefly possible numerical methods for getting approximate energy levels.

The dipole polarizability of helium is another fundamental property of this prototypical two-electron system whose accurate calculation has generated much interest (see, e.g., Refs. [16–27]). A comprehensive review on electric dipole polarizabilities for atoms has been given by Bonin and Kadar-Kallen [28]. As pointed out in that review, polarizabilities are important in a number of areas in physics and chemistry, such as interactions between matter and electromagnetic fields, collision phenomena, and others. Many physical properties are related to the polarizability, as for instance the dielectric constant and refractive index. Owing to such a broad interest in determining polarizabilities, many theoretical methods have been employed. However, many fewer highly accurate methods exist for polarizabilities than for energies. An interesting fact, recently shown by Pachucki and Sapirstein [27], is that the mass polarization, relativistic, and QED corrections to the nonrelativistic static polarizability cancel almost completely, giving a contribution to the He static polarizability of under 2 ppm. This accidental cancellation highlights the importance of highly accurate calculations of the polarizability in the nonrelativistic limit in order to test the effect of these higher-order corrections. Although many different methods and techniques exist, only a few of them are able to give the requisite precision. Significantly, none of the many prior calculations include logarithmic terms in their formulation.

We present, in addition to energy levels, a calculation of the static and dynamic dipole polarizability of the helium atom using a variationally stable, coupled-channel hyperspherical approach [20,29–32], in which the initial- and intermediate-state wave functions are represented by Fock expansions [1,2,33–36]. Our results include logarithmic terms in the wave-function expansions in order to calculate an observable other than the energy. In the calculation of energy levels, those terms have served only to speed up the convergence of the result (see, e.g., Refs. [4,5]). On the contrary, in our calculation of the dipole polarizability, the logarithmic terms play a crucial role in obtaining accurate values when using nonoptimized parameters in the intermediate-state functions. When an optimization procedure is included, the logarithmic terms become less important, at the expense of more CPU time. Comparing the results we obtain both with and without the logarithmic terms for the static polarizability, we are able to demonstrate their important role for the hyperspherical basis we employ. The present approach, in which we treat up to 12 coupled $^1S^e$ channels and up to 15 coupled $^1P^o$ channels, is able to furnish five digits of accuracy for polarizabilities. While this level of accuracy is unable to provide benchmark results for the He static polarizability (since the best results of others give seven or more digits of accuracy), our method is nevertheless more than sufficient to provide competitive results for the dynamical polarizabilities as well as for our next main goal, the calculation of multiphoton cross sections with an accuracy exceeding that of current experimental capabilities.

This paper is structured as follows. In Sec. II we summarize the theoretical aspects of the present approach, giving the fundamental equations. Section III gives some details regarding the numerical and calculational features of our ap-

 ©2003 The American Physical Society

proach. In Sec. IV we present the results for the static and frequency-dependent dipole polarizabilities as well as for the energies; we provide also an analysis of the convergence of our results. In addition, comparisons with other results in literature are given. Finally, Sec. V presents our conclusions and some perspectives.

II. THE VARIATIONALLY STABLE, COUPLED-CHANNEL HYPERSPHERICAL APPROACH

For two-electron systems, such as helium and its isoelectronic series, the hyperspherical coordinate representation is very suitable for describing the wave functions (see Ref. [37] for a review on this subject). The set of coordinates employed is $\{R,\alpha,\theta_1,\phi_1,\theta_2,\phi_2\}$, where $R=(r_1^2+r_2^2)^{1/2}$, $\alpha=\tan^{-1}(r_1/r_2)$, and θ_i, ϕ_i are the usual angular coordinates.

The matrix element for a two-photon transition between an initial state $|i\rangle$ and a final state $|f\rangle$ is written as

$$T^{(2)}_{i\to f}(\omega)=\left\langle f\left| D\frac{1}{E_i+\omega-\hat{H}}D\right| i\right\rangle, \tag{1}$$

where $D=\boldsymbol{\epsilon}\cdot(\mathbf{r}_1+\mathbf{r}_2)$ is the length form of the electric dipole operator, E_i is the energy of the initial state, $\boldsymbol{\epsilon}$ is the light polarization vector, and ω is the photon energy. The variationally stable form of Eq. (1), according to Refs. [20,29–31], is

$$T^{(2)}_{i\to f}(\omega)=\langle f|D|\lambda\rangle+\langle\lambda'|D|i\rangle-\langle\lambda'|E_i+\omega-\hat{H}|\lambda\rangle, \tag{2}$$

where $|\lambda\rangle$ and $\langle\lambda'|$ represent unknown functions related to $|i\rangle$ and $\langle f|$, respectively, by a one-photon transition. The two-photon transition rate in Eq. (2) is variationally stable in the sense that it depends only quadratically on errors in the determination of $|\lambda\rangle$ and $\langle\lambda'|$ [30]. In Eq. (2), the Hamiltonian in hyperspherical coordinates is given by (atomic units are used throughout this paper)

$$\hat{H}=-\frac{1}{2}\left(\frac{\partial^2}{\partial R^2}+\frac{\hat{U}(R,\Omega)+1/4}{R^2}\right), \tag{3}$$

and the operator $\hat{U}(R,\Omega)$ is the angular part of the Hamiltonian, with a parametric dependence on R,

$$\hat{U}(R,\Omega)=\frac{\partial^2}{\partial\alpha^2}-\frac{\hat{L}_1^2}{\sin^2\alpha}-\frac{\hat{L}_2^2}{\cos^2\alpha}+\frac{2ZR}{\sin\alpha}+\frac{2ZR}{\cos\alpha}-\frac{2R}{\sqrt{1-\sin(2\alpha)\cos\theta_{12}}}, \tag{4}$$

where $\hat{L}_1^2$ and $\hat{L}_2^2$ are the usual angular-momentum operators of the individual electrons and θ_{12} is the angle between their position vectors: $\cos\theta_{12}=\hat{\mathbf{r}}_1\cdot\hat{\mathbf{r}}_2$. An eigenvalue equation for the operator $\hat{U}(R,\Omega)$, i.e.,

$$\hat{U}(R,\Omega)\Phi_\mu(R;\Omega)=U_\mu(R)\Phi_\mu(R;\Omega), \tag{5}$$

furnishes a set of channel functions $\Phi_\mu(R;\Omega)$ and a set of corresponding potential curves $U_\mu(R)$, where the index μ is a collective label for all relevant quantum numbers. At $R=0$, Eq. (5) is exactly solvable and the solutions can be written in terms of Jacobi polynomials with the corresponding eigenvalues given by

$$U_\mu(0)=-(l_1+l_2+2\tilde{n}+2)^2, \tag{6}$$

where l_1 and l_2 are the individual angular-momentum quantum numbers of the electrons and $\tilde{n}$ is the degree of the Jacobi polynomial of a particular solution. It represents the number of nodes in α (at $R=0$) of a given channel.

The initial- and final-state wave functions as well as the functions λ and λ' are expanded in adiabatic hyperspherical channel functions [20,38,31]; they all have similar forms:

$$\Psi(R,\Omega)=(R^{5/2}\sin\alpha\cos\alpha)^{-1}\sum_\mu F_\mu(R)\Phi_\mu(R;\Omega), \tag{7}$$

$$\lambda(R,\Omega)=(R^{5/2}\sin\alpha\cos\alpha)^{-1}\sum_\nu \lambda_\nu(R)\Phi_\nu(R;\Omega), \tag{8}$$

$$\lambda'(R,\Omega)=(R^{5/2}\sin\alpha\cos\alpha)^{-1}\sum_\mu \lambda'_\mu(R)\Phi_\mu(R;\Omega), \tag{9}$$

where the expansion coefficients $F_\mu(R)$ satisfy the coupled radial equations

$$\left(\frac{d^2}{dR^2}+\frac{U_\mu(R)+1/4}{R^2}+2E\right)F_\mu(R)+\sum_\nu\left[2P_{\mu\nu}(R)\frac{d}{dR}+Q_{\mu\nu}(R)\right]F_\nu(R)=0, \tag{10}$$

and $\lambda_\nu(R)$ and $\lambda'_\mu(R)$ are determined by the variational procedure described below. The coupling terms in Eq. (10) are known as nonadiabatic couplings and are defined by

$$P_{\mu\nu}(R)=\left\langle\Phi_\mu\left|\frac{d}{dR}\right|\Phi_\nu\right\rangle \tag{11}$$

and

$$Q_{\mu\nu}(R)=\left\langle\Phi_\mu\left|\frac{d^2}{dR^2}\right|\Phi_\nu\right\rangle, \tag{12}$$

where the brackets mean integration over the angular variables Ω. In order to evaluate the radial integrals of Eq. (2), we expand the unknown radial functions as

$$\lambda_\nu(R)=\sum_{i=1}^{B_{\max}}\sum_{j=1}^{M_i}a_{ij}^\nu\phi_{ij}^\nu(R) \tag{13}$$

and

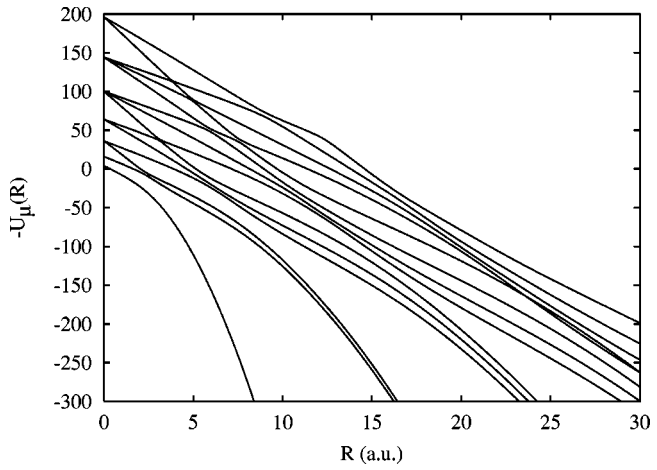

FIG. 1. Set of potential curves $-U_\mu(R)$ for $^1S^e$ states of the helium atom.

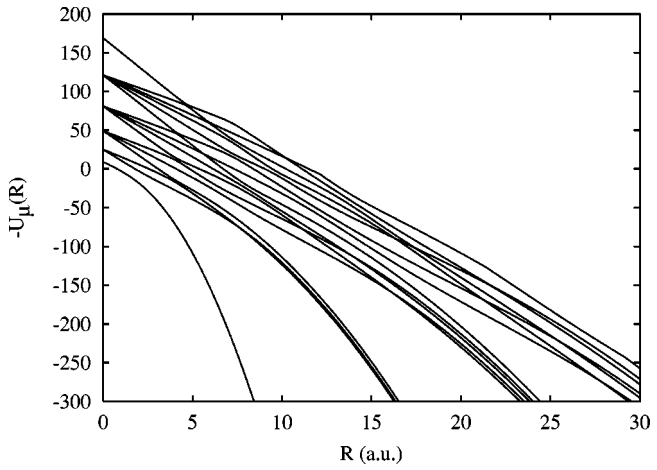

FIG. 2. Same as Fig. 1 for $^1P^o$ states.

$$\lambda'_\mu(R)=\sum_{i'=1}^{B_{\max}}\sum_{j'=1}^{M_{i'}} b^\mu_{i'j'}\theta^\mu_{i'j'}(R), \tag{14}$$

where $\phi^\nu_{ij}(R)$ and $\theta^\mu_{i'j'}(R)$ are chosen to be modified Slater orbitals that include powers of $\ln R$, i.e.,

$$\phi^\nu_{ij}(R)=N^\nu_{i,j+2(i-1)}R^{S^\nu_{ij}}(\ln R)^{i-1}e^{-\beta^\nu_i R} \tag{15}$$

and

$$\theta^\mu_{i'j'}(R)=N^\mu_{i',j'+2(i'-1)}R^{S^\mu_{i'j'}}(\ln R)^{i'-1}e^{-\beta^\mu_{i'}R}, \tag{16}$$

where $N^\mu_{i,j}$ is a normalization constant for the i,j basis function of each channel μ and the exponents of R are given by $S^\mu_{ij}=\sqrt{-U_\mu(0)}+1/2+j+2(i-1)$ (cf. Ref. [35]). The constants β^μ_i are free parameters whose determination is described in Sec. III.

The frequency-dependent polarizability is calculated using the second-order transition matrix element as follows:

$$\alpha(\omega)=-[T^{(2)}_{i\to i}(+\omega)+T^{(2)}_{i\to i}(-\omega)], \tag{17}$$

where the final state $|f\rangle$ is replaced by the initial state $|i\rangle$ in Eq. (2). In the static limit, i.e., the photon frequency $\omega\to 0$, the expression for the polarizability reduces to a simpler form: $\alpha(0)=-2T^{(2)}_{i\to i}(0)$.

III. CALCULATIONAL ASPECTS

In this section, we discuss the numerical aspects of our calculations. It should be stressed here that these are numerically intensive calculations, particularly because our codes use REAL*16 (quadruple) precision in order to minimize numerical error propagation and to deal accurately with a mix of both small and large numbers.

In Eqs. (7)–(12), the channel indices μ and ν run from 1 to a maximum number N_c of coupled channels that are considered in the adiabatic expansions. The positive constants β^μ_i, introduced through the Slater basis functions in Eqs. (15) and (16), can be heuristically chosen: the starting trial values for the β^μ_i are chosen to be close to the value $\sqrt{-2E_0}$, where $-E_0=0.903\,724$ a.u. is the electron binding energy for the helium atom. Then, a spread of values around the initial trial values are investigated and their convergence properties and stability are examined with the aim of minimizing error propagation. In this work, we have also developed an optimization procedure for searching for the best set of β^μ_i parameters. This procedure is based on the minimization of the transition matrix element [Eq. (2)] with respect to β^μ_i. Note that for photon frequencies above the ionization threshold, β^μ_i should be chosen to be complex in order to correctly describe the oscillatory character of the intermediate-state continuum wave functions.

The hyperspherical method focuses on the determination of potential curves and the corresponding channel functions [see Eq. (5)]. Due to the nature of the angular operator [Eq. (4)], the solution of Eq. (5) is the most difficult step of the method. Nevertheless, the angular operator $\hat{U}(R,\Omega)$ is not dependent on the system's energies, which means that the set of potential curves and nonadiabatic couplings are calculated a single time for the system under consideration. Due to the symmetry breaking caused by the electron-electron repulsion, the angular operator is not separable and Eq. (5) becomes an angular coupled channel equation [38]. In solving this eigenvalue equation, we have used an expansion in the individual angular momenta of the electrons [35]. The coupled-channel expansions have been truncated at the maximum value $l_1^{\max}=l_2^{\max}=9$ for the $^1S^e$ and $^1P^o$ channels with the exception of the lowest potential curves of each symmetry. These potential curves are the most important ones since they support the bound states. For the first $^1S^e$ potential curve, 40 components of angular momentum have been included, i.e., $l_1^{\max}=l_2^{\max}=39$ and for the first $^1P^o$ potential curve, 60 components have been used, i.e., $l_1^{\max}=l_2^{\max}=30$. Bound and scattered states are obtained using proper boundary conditions in solving the radial equations. In the calculation of static and dynamic polarizabilities (taking the initial state as the ground state), potential curves for both $^1S^e$ and $^1P^o$ states are required.

TABLE I. Ground-state energy convergence as a function of the number N_c of coupled radial equations. The error is relative to the variational value of Frankowski and Pekeris [4]. The first row, with $N_c=1$, corresponds to the calculation in which all couplings are neglected, giving a lower-energy bound; the second row, also with $N_c=1$, corresponds to the one in which only the diagonal coupling matrix element is taken into account, giving an upper-energy bound. Horizontal lines delimit groups of channels (see text).

N_c	$(l_1,l_2,\tilde{n};n)$	E_i (a.u.)	$(E_{\rm var}-E_i)/E_{\rm var}$ (ppm)
1	(0,0,0;1)	−2.930 032 616	−9 060.171
1	(0,0,0;1)	−2.895 554 014	2 813.753
2	(1,1,0;2)	−2.898 646 614	1 748.707
3	(0,0,2;2)	−2.903 611 486	38.878
4	(2,2,0;3)	−2.903 632 473	31.650
5	(1,1,2;3)	−2.903 636 415	30.293
6	(3,3,0;3)	−2.903 658 492	22.690
7	(0,0,4;4)	−2.903 717 088	2.510
8	(2,2,2;4)	−2.903 717 136	2.494
9	(4,4,0;4)	−2.903 717 238	2.459
10	(1,1,4;4)	−2.903 717 274	2.446
11	(3,3,2;5)	−2.903 717 376	2.411
12	(5,5,0;5)	−2.903 717 997	2.197
13	(0,0,6;5)	−2.903 722 980	0.481
14	(2,2,4;5)	−2.903 723 027	0.465
Variational value [4]		−2.903 724 377	

IV. RESULTS

The potential curves used in our calculations are shown in Figs. 1 and 2, where the $R=0$ degeneracy is evident and exact, according to Eq. (6). The degenerate curves suggest a natural grouping of channels, which will prove relevant for analyzing the convergence of our results as a function of the number of channels included in our calculations. Note the apparent crossings between contiguous curves, especially for the higher ones. In fact, those are avoided-crossing regions, where the corresponding channel functions suddenly ex-

TABLE II. Same as Table I, for the $1s2p\ ^1P^o$ state, where the error is relative to the variational value of Schiff *et al.* [43]. Horizontal lines delimit groups of channels (see text).

N_c	$(l_1,l_2,\tilde{n};n)$	E_i (a.u.)	$(E_{\rm var}-E_i)/E_{\rm var}$ (ppm)
1	(0,1,0;1)	−2.145 599 305	−10 243.798
1	(0,1,0;1)	−2.121 696 638	1 010.643
2	(0,1,1;2)	−2.123 010 231	392.145
3	(1,2,0;2)	−2.123 219 358	293.679
4	(0,1,2;2)	−2.123 611 967	108.821
5	(1,2,1;3)	−2.123 621 908	104.141
6	(2,3,0;3)	−2.123 645 237	93.156
7	(0,1,3;3)	−2.123 734 421	51.165
8	(1,2,2;3)	−2.123 738 246	49.363
9	(2,3,1;3)	−2.123 750 987	43.365
10	(3,4,0;4)	−2.123 755 209	41.377
11	(0,1,4;4)	−2.123 790 757	24.639
12	(1,2,3;4)	−2.123 792 018	24.045
13	(2,3,2;4)	−2.123 794 936	22.671
14	(3,4,1;4)	−2.123 797 519	21.455
15	(4,5,0;4)	−2.123 798 539	20.975
16	(0,1,5;4)	−2.123 811 116	15.053
Variational value [43]		−2.123 843 086	

TABLE III. Static polarizability of the helium atom using five-β Slater basis functions without and with logarithmic terms (for $N_c = N_c'$), where N_c is the number of coupled channels. The difference between the two rows with $N_c=1$ is explained in the caption of Table I. The results for $\alpha(0)$ in columns 4 and 5 do not involve optimized values of the β_i^μ parameters; those in columns 6 and 7 do.

			$\alpha(0)$			
N_c	S state $(l_1,l_2,\tilde{n};n)$	P state $(l_1,l_2,\tilde{n};n)$	Neglecting log terms [a]	Including log terms [a]	Optimized without log terms [b]	Optimized with log terms [c]
1	(0,0,0;1)	(0,1,0;1)	1.386 392	1.386 392		
1	(0,0,0;1)	(0,1,0;1)	1.394 070	1.394 070	1.394 068 70	1.394 068 70
2	(1,1,0;2)	(0,1,1;2)	1.381 100	1.395 580	1.395 576 02	1.395 576 03
3	(0,0,2;2)	(1,2,0;2)	1.356 458	1.380 733	1.380 730 90	1.380 731 32
4	(2,2,0;3)	(0,1,2;2)	1.387 758	1.383 117	1.383 116 07	1.383 116 44
5	(1,1,2;3)	(1,2,1;3)	1.387 457	1.382 986	1.382 973 07	1.382 973 12
6	(3,3,0;3)	(2,3,0;3)	1.387 635	1.383 227	1.383 225 32	1.383 225 55
7	(0,0,4;4)	(0,1,3;3)	1.392 171	1.383 045	1.383 066 40	1.383 067 30
8	(2,2,2;4)	(1,2,2;3)	1.393 330	1.383 086	1.383 068 82	1.383 069 73
9	(4,4,0;4)	(2,3,1;3)	1.392 195	1.383 067	1.383 069 74	1.383 070 43
10	(1,1,4;4)	(3,4,0;4)	1.392 073	1.383 094	1.383 074 42	1.383 074 30
11	(3,3,2;5)	(0,1,4;4)	1.397 085	1.383 163	1.383 152 43	1.383 152 73
12	(5,5,0;5)	(1,2,3;4)	1.391 545	1.383 193	1.383 162 64	1.383 162 94

[a]Five nonoptimized β_i^μ parameters.
[b]One β_i^μ parameter. Results from Table IV.
[c]Two β_i^μ parameters.

change their behaviors, resulting in sharp peaks in the nonadiabatic couplings due to the first and second derivatives present in their definitions, as seen in Eqs. (11) and (12).

For reasons of consistency, the ground-state energy E_i used in Eq. (1) is the calculated hyperspherical value for the number of channels included in our calculations, as shown in Table I. In this table, as the number of coupled channels increases, the corresponding calculated energy approaches the variational value of Ref. [4]. The first row with $N_c=1$ corresponds to the calculation in which all couplings are neglected, giving a lower bound for the energy [39,40]. The second row with $N_c=1$ corresponds to the calculation in which only the diagonal coupling is taken into account. This value, and all subsequent ones, are upper-energy bounds [39,40]. The second column lists the $R=0$ angular quantum numbers [see Eq. (6)] as well as the asymptotic hydrogenic threshold n; this set of numbers labels each potential curve (and the corresponding angular channel). For second-order processes such as the dipole polarizability of the ground state, the intermediate states possess symmetry $^1P^o$. For this reason, Table II is included in order to analyze the convergence of the $1s2p$ energy. One sees in Table I that as additional adiabatic hyperspherical channels are included in our calculations, the deviations from the variational value of Ref. [4] decrease monotonically. Large decreases occur when the hyperspherical channels that converge to $n=2$ ($N_c=2$, 3), $n=3$ ($N_c=4$, 5, 6), and the first channel converging to $n=4$ ($N_c=7$) are included. The largest decreases occur when the last channel included has an angular function containing s waves (i.e., electron orbital angular momenta $l_1=l_2=0$) at $R=0$; this occurs for $N_c=3$, 7, and 13. A similar pattern can be found in Table II for the $1s2p$ state. In both Tables I and II, horizontal lines delimit groups of channels. Inside each group the convergence is steady but slow. One could also try grouping of channels using the asymptotic threshold n as a parameter. We believe that grouping of channels using their $R=0$ characters is the most appropriate method since the corresponding potential wells [see Eq. (3)] are in the small- and mid-R regions and, consequently, in this region the channel functions are better characterized by their $R=0$ behaviors than by their $R\to\infty$ behaviors. As noted from Tables I and II, a new group of channels starts when an angular channel with an $l_1=0$ component is included. Note how every time a new channel having $l_1=0$ is included, the error drops dramatically. This behavior (and its associated channel grouping) will prove useful for analyzing the convergence of the static polarizability, for which both $^1S^e$ and $^1P^o$ symmetries are involved.

A. Static polarizability

In our calculation of the static polarizability without the optimization of the exponential parameters β_i^μ, our expansions of the radial functions in Eqs. (15) and (16) include factors such as $R^{S_{i0}^\mu+j}(\ln R)^{i-1}$, where $1\leqslant i\leqslant B_{\max}$ and $1\leqslant j\leqslant M_i$ so that $B_{\max}-1$ is the highest power of $\ln R$ and $M_i+S_{i0}^\mu$ is the highest power of R for a given power $(i-1)$ of $\ln R$. We have used in the expansions of Eqs. (13) and (14), $B_{\max}=5$ with $\beta_1^\mu=0.3$, $\beta_2^\mu=0.5$, $\beta_3^\mu=0.8$, $\beta_4^\mu=1.2$, and $\beta_5^\mu=1.7$. For each value of β_i^μ, $M_i=M=12$, although $M=8$ or even $M=6$ suffices to obtain reasonable precision. Although for H^- we have found that $B_{\max}=1$ suffices [32], which implies the absence of logarithmic terms in

TABLE IV. Convergence for the calculated static dipole polarizability of the helium atom as a function of the number of coupled channels for the initial ground state (N_c) and for the intermediate states (N_c'). Calculations employ one optimized β_i^μ parameter. Horizontal and vertical lines delimit groups of channels (see text).

	N_c													
N_c'	1	2	3	4	5	6	7	8	9	10	11	12	13	14
1	1.394 069	1.353 977	1.324 336	1.324 337	1.324 098	1.324 162	1.323 510	1.323 511	1.323 510	1.323 504	1.323 510	1.323 519	1.323 460	1.323 460
2	1.427 833	1.395 576	1.380 032	1.379 974	1.379 764	1.379 803	1.379 160	1.379 160	1.379 160	1.379 154	1.379 159	1.379 169	1.379 110	1.379 110
3	1.428 627	1.395 777	1.380 731	1.380 723	1.380 515	1.380 555	1.379 910	1.379 911	1.379 910	1.379 905	1.379 910	1.379 919	1.379 861	1.379 861
4	1.431 625	1.398 484	1.383 111	1.383 116	1.382 930	1.382 980	1.382 345	1.382 346	1.382 345	1.382 340	1.382 345	1.382 354	1.382 297	1.382 297
5	1.431 669	1.398 502	1.383 140	1.383 149	1.382 973	1.383 022	1.382 387	1.382 388	1.382 387	1.382 382	1.382 387	1.382 397	1.382 341	1.382 341
6	1.431 888	1.398 665	1.383 275	1.383 302	1.383 126	1.383 225	1.382 588	1.382 589	1.382 588	1.382 583	1.382 588	1.382 598	1.382 543	1.382 543
7	1.432 474	1.399 150	1.383 652	1.383 672	1.383 483	1.383 645	1.383 066	1.383 067	1.383 066	1.383 061	1.383 066	1.383 076	1.383 021	1.383 021
8	1.432 479	1.399 152	1.383 655	1.383 675	1.383 484	1.383 647	1.383 068	1.383 069	1.383 068	1.383 063	1.383 068	1.383 077	1.383 023	1.383 023
9	1.432 480	1.399 153	1.383 656	1.383 676	1.383 485	1.383 648	1.383 070	1.383 070	1.383 070	1.383 064	1.383 070	1.383 079	1.383 024	1.383 024
10	1.432 484	1.399 158	1.383 660	1.383 680	1.383 490	1.383 658	1.383 079	1.383 080	1.383 080	1.383 074	1.383 080	1.383 089	1.383 034	1.383 034
11	1.432 585	1.399 247	1.383 736	1.383 756	1.383 565	1.383 737	1.383 152	1.383 153	1.383 152	1.383 147	1.383 152	1.383 162	1.383 107	1.383 107
12	1.432 586	1.399 247	1.383 736	1.383 756	1.383 566	1.383 738	1.383 153	1.383 153	1.383 153	1.383 148	1.383 153	1.383 163	1.383 108	1.383 108
13	1.432 588	1.399 249	1.383 738	1.383 757	1.383 567	1.383 739	1.383 154	1.383 155	1.383 154	1.383 149	1.383 155	1.383 164	1.383 109	1.383 109
14	1.432 590	1.399 250	1.383 739	1.383 759	1.383 568	1.383 740	1.383 155	1.383 156	1.383 155	1.383 150	1.383 156	1.383 165	1.383 110	1.383 110
15	1.432 601	1.399 259	1.383 747	1.383 767	1.383 576	1.383 747	1.383 162	1.383 163	1.383 162	1.383 157	1.383 164	1.383 174	1.383 119	1.383 119
16	1.432 621	1.399 278	1.383 763	1.383 783	1.383 593	1.383 764	1.383 179	1.383 179	1.383 179	1.383 174	1.383 196	1.383 208	1.383 157	1.383 157

TABLE V. Comparison of the present variationally stable results for the ground-state static dipole polarizability of the He atom with theoretical results of other authors and available experimental values. The result in the first line was calculated using $N_c = N_c' = 12$, whereas the two subsequent lines show results using $N_c = 12$ and $N_c' = 15$.

Reference	$\alpha(0)$
Theoretical results	
This work (coupled-channel result including log terms[a])	1.383 193
This work (optimized coupled-channel result without log terms[b])	1.383 173 59
This work (optimized coupled-channel result including log terms[c])	1.383 173 94
K. Pachucki and J. Sapirstein (2000) (Ref. [27])	1.383 192 174
Z.-C. Yan *et al.* (1996) (Ref. [25])	1.383 192 5
M. J. Jamieson, G. W. F. Drake, and A. Dalgarno (1995) (Ref. [24])	1.383 192
A. K. Bhatia and R. J. Drachman (1994) (Ref. [23])	1.383 192 179
D. M. Bishop and J. Pipin (1993) (Ref. [22])	1.383 192
D. M. Bishop and B. Lam (1988) (Ref. [19])	1.383 192
R. M. Glover and F. Weinhold's *lower* bound (1976) (Ref. [17])	1.382 59
R. M. Glover and F. Weinhold's *upper* bound (1976) (Ref. [17])	1.384 11
S. J. A. van Gisbergen *et al.* (1998) (Ref. [26])	1.382 4
H. P. Saha and C. D. Caldwell (1991) (Ref. [21])	1.374
B. Gao *et al.* (1990) (Ref. [20])	1.355 9
E.-A. Reinsch (1985) MC-SCF result (Ref. [18])	1.383
K. T. Chung (1968) (Ref. [16])	1.384 1
Experimental results	
C. R. Mansfield and E. R. Peck (1969) (Ref. [44])	1.386 1
P. W. Langhoff and M. Karplus (1969) (Ref. [45])	1.383 8
D. Gugan and G. W. Michel (1980) (Ref. [46])	1.383 77(7)
D. Gugan (1991) (Ref. [47])	1.383 79(4)
K. Grohmann and H. Luther (1992) (Ref. [48])	1.383 746(7)

[a]Five nonoptimized β_i^μ parameters, $N_c = N_c' = 12$ channels (cf. Table III).
[b]One optimized β_i^μ parameter, $N_c = 12$, $N_c' = 15$ channels (cf. Table IV).
[c]Two optimized β_i^μ parameters, $N_c = 12$, $N_c' = 15$ channels.

the intermediate-state functions, for the helium atom we discovered that not only should $B_{\max}$ be greater than unity but also that it needs to be at least greater than or equal to three in order to obtain convergence to the correct value of the static polarizability. In the adiabatic approximation, where $N_c = 1$, the three matrix elements in Eq. (2) are equal to each other (to ten digits of accuracy). For the nonadiabatic coupled-channel calculation, i.e., $N_c \geqslant 2$, they are typically converged to within five or six digits of accuracy. We regard the accuracies of these equalities as indicators of the level of accuracy of our results. Note also that for these calculations we have not altered the parameters as the number of channels is increased; doing so may be necessary for larger numbers of channels, as these correspond to higher-energy levels of He^+.

Table III lists the calculated values of the static polarizability according to Eq. (17), with $\omega = 0$, as the number of coupled channels increases. The quantum numbers that label the potential curves, listed in Tables I and II, are also included to help identify the groups of channels. This table lists the values obtained by neglecting the logarithmic terms in Eqs. (15) and (16) alongside the results obtained by including the logarithmic terms. Other than the inclusion or exclusion of the logarithmic terms, both calculations were otherwise the same. That is, they used the same parameters (such as the number of β_i^μ constants) and the same number of basis functions. Comparison of the two variational calculations clearly indicates the importance of the use of the logarithmic expansion. They are important not only for accelerating the convergence but also for obtaining the correct value. Note that in calculating the polarizability there are two sets of coupled channels: the $^1S^e$ channels, which couple to the ground state, and the $^1P^o$ channels which constitute the intermediate states. One sees from Table III that the convergence is not a monotonically decreasing function of the number N_c of coupled channels. An interesting question is whether the convergence would become smoother if different numbers of channels were coupled in ground and intermediate states. For example, one might include all hyperspherical channels that converge to a particular level n of the He^+ ion in both ground and intermediate states. Alternatively, one might group the various adiabatic hyperspherical channels in some other way, such as according to their character at $R = 0$. We have carried out this study coupling all available channels in ground and intermediate states. In Table IV, we study the convergence of the static polarizability as a function of N_c and N_c', which are the numbers of coupled channels in both ground and intermediate states, respectively, where we have used for this purpose a single β_i^μ, which

TABLE VI. Selected values of our best calculated ($N_c = N_c' = 6$) dynamic polarizability of helium compared with results from other authors and with experimental values.

ω	This work	Ref. [16]	Ref. [17]	Ref. [18]	Ref. [19]	Expt.[a]
0.050	1.387 094	1.386 8	1.387 22		1.387 066	
0.100	1.398 857	1.399 0	1.398 98	1.398	1.398 820	1.399
0.150	1.418 998	1.419 2	1.419 12		1.418 957	
0.200	1.448 388	1.448 3	1.448 51	1.448	1.448 341	1.449
0.250	1.488 389	1.488 7	1.488 53		1.488 335	
0.300	1.541 045	1.540 7	1.541 19	1.540	1.540 981	1.542
0.350	1.609 399	1.609 5	1.609 56		1.609 325	
0.400	1.698 070	1.698 0	1.698 3	1.696	1.697 985	1.700
0.450	1.814 308	1.814 7	1.814 5		1.814 214	
0.500	1.970 129	1.970 6	1.970 5	1.966	1.970 037	1.973
0.550	2.187 047	2.187 2	2.187 5	2.182	2.186 990	
0.600	2.508 200	2.509 1	2.509 1	2.501	2.508 292	2.502
0.650	3.036 655	3.038 0	3.039 1	3.022	3.037 345	
0.700	4.107 153	4.110 3	4.118 4	4.079	4.111 021	3.884
0.750	7.967 789	7.968 4	8.164 0	7.967	8.014 127	
0.770	17.070 652	16.866 8				
0.780	1 765.866 727	56.096 9	−1 073.68			
0.782	−90.326 704	116.456 0				
0.784	−42.857 302	−968.839 5				
0.785	−33.466 465		−31.46			
0.790	−14.990 171	−30.746 1	−14.56			
0.795	−8.852 173		−8.71			
0.800	−5.722 310	−10.329 0	−5.66			
0.805	−3.768 979		−3.75			
0.810	−2.380 470		−2.38			
0.815	−1.286 429		−1.30			
0.820	−0.336 927		−0.37			
0.825	0.578 338		0.52			
0.830	1.581 768		1.47			
0.835	2.894 517		2.65			
0.840	5.173 656		4.52			
0.845	12.633 684		9.75			

[a]Reference [18].

means that the basis functions do not include logarithmic terms. The horizontal and vertical lines correspond to the horizontal lines of Tables I and II, i.e., they show the beginning of each group of channels, where each group begins with a channel having $l_1 = 0$ at $R = 0$ [see Eq. (6)]. In our calculations for $\alpha(0)$, we have introduced an optimization procedure for the parameters β_i^μ. The optimal set of β_i^μ parameters is found by minimizing the transition matrix element [Eq. (2)] with respect to each β_i^μ. Table III lists the results using optimized β_i^μ in the intermediate functions. A side-by-side comparison shows that only a single optimized value for the β_i^μ parameter is sufficient to achieve results very close to the ones obtained with five nonoptimized β_i^μ parameters and logarithmic terms. On the other hand, additional CPU time is required for the optimization procedure. Anticipating that readers will wish to know what would happen if one combines the inclusion of logarithmic terms together with the optimization of the β_i^μ, a sample for the first few coupled channels have been computed and displayed in the last column of Table III. One sees that the improvement is beyond the sixth or seventh decimal digit, with a high cost in terms of computer resources.

Some information about the convergence of the calculated $\alpha(0)$ value with the number of channels can be extracted from Table IV. For each column, the same convergence pattern of $^1P^o$ states, shown in Table II, is found as N_c' increases. Within each group of channels the polarizability increases slowly and monotonically whereas larger increments occur when a new group is included. A different pattern is noted when looking at the rows, which show the convergence as the number N_c of channels included in the ground-state wave function is increased. Within each group the convergence oscillates with increasing N_c. However, the important feature is that considering only the values obtained with a *complete group* of N_c channels included, the results are monotonically decreasing. These results are represented

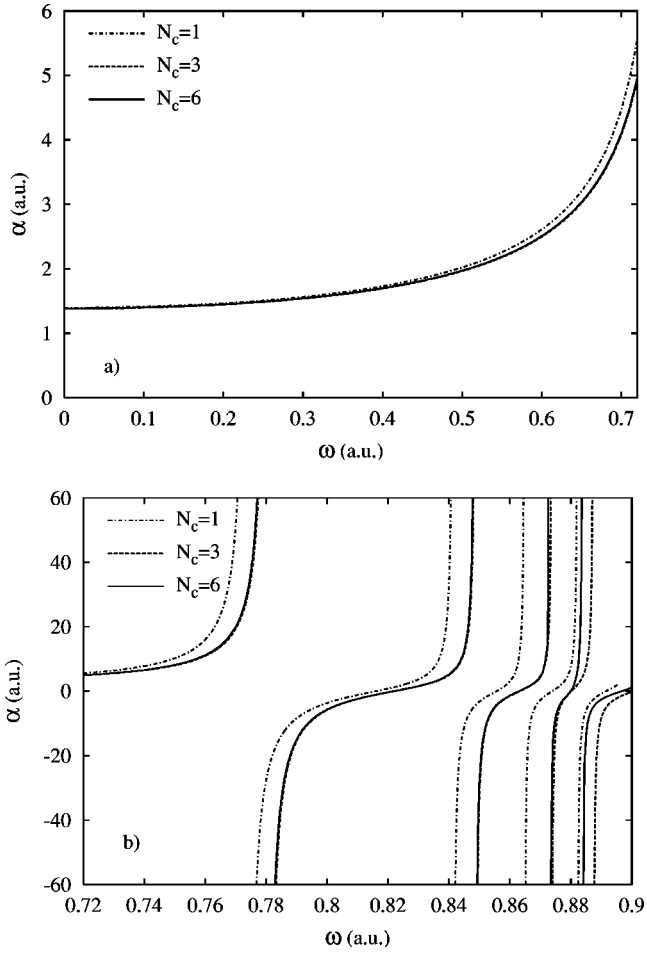

FIG. 3. Convergence of the dynamic polarizability of helium for photon frequencies below the first ionization threshold. (a) Below the first excitation frequency. (b) Resonance region.

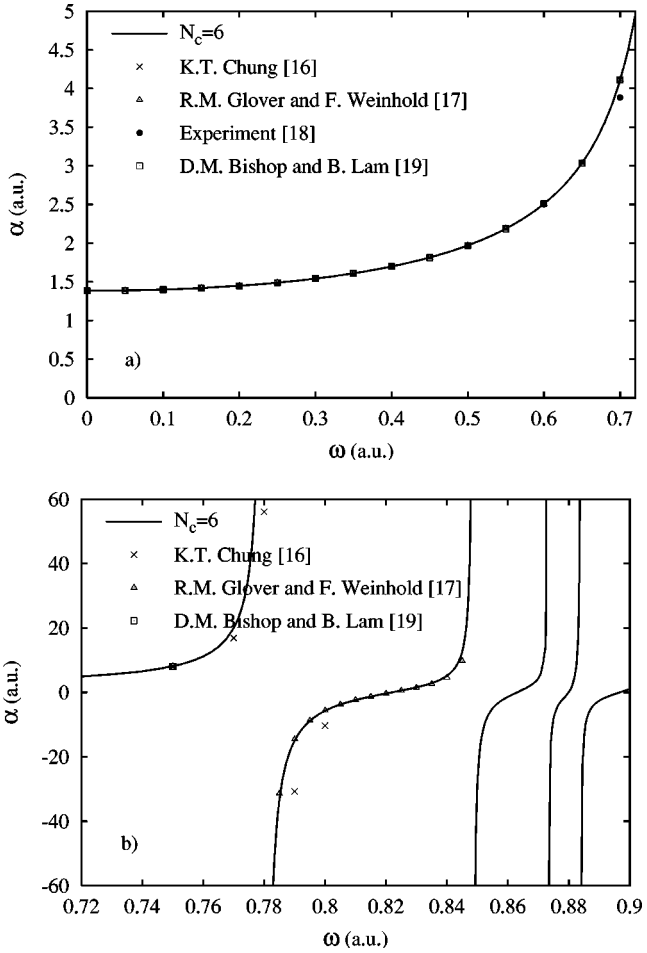

FIG. 4. Comparison of our best result for the dynamic polarizability of helium with other theoretical calculations and with experimental values. (a) Below the first excitation frequency. (b) Resonance region.

by the values to the immediate left of the vertical lines. The numbers inside the boxes are the results after complete groups of channels in both ground and intermediate states are included. Thus, this analysis relates the convergence pattern of the polarizability with the behavior of the $^1S^e$ and $^1P^o$ energy convergence, shown in Tables I and II. The convergence with N_c should be examined for entire groups of channels and the convergence with N_c' is monotonic and consequently one does not need to group channels, although one should expect jumps at the beginning of a new group. To further investigate the convergence and reliability of our results, an extrapolation procedure can be used. If one takes into account solely the results inside boxes from Table IV, each row and column can be fitted to a function of the type

$$\alpha(x) = a + \frac{b}{x^c}, \tag{18}$$

whence one can extrapolate to an infinite number of groups in both directions. This extrapolation procedure may be done in two ways: starting by rows or by columns. Within six digits of accuracy, the resulting values are $\alpha_{\text{ext}} = 1.383\,18$ and $\alpha_{\text{ext}} = 1.383\,10$, respectively. Comparing these two extrapolated values with our result of $\alpha = 1.383\,174$ ($N_c = 12$ and $N_c' = 15$), we can assure a convergence of at least five digits. It is remarkable how our method is capable of providing results for polarizabilities that possess almost the same level of accuracy as for the ground-state energy (cf. Table I, $N_c = 12$), which is usually not true.

In Table V, a comparison of our coupled channel values with the results of calculations of other authors and with experimental values is given. Our result using one optimized β_i^μ without logarithmic terms ($N_c = 12$ and $N_c' = 15$) and five nonoptimized β_i^μ including logarithmic terms ($N_c = N_c' = 12$) are presented. We also show the result of two optimized β_i^μ plus inclusion of logarithmic terms ($N_c = 12$ and $N_c' = 15$). As noted before, the improvement in the latter is beyond the sixth decimal digit. Not all of the results of others lie between the rigorous bounds from Glover and Weinhold [17]. Our results fall between these limits. Indeed, our precise results are comparable to the most accurate ones from the literature, such as that of Ref. [27]. Among the various theoretical calculations, the works by Bishop and co-workers [19,22], Bhatia and Drachman [23], Jamieson *et al.* [24], and Pachucki and Sapirstein [27] appear to be the most accurate

TABLE VII. Comparison of the one-photon transition resonances extrapolated from Fig. 4(b) with results in the literature.

This work[a]	Variational[b]	Hyperspherical[c]
0.780 100	0.779 881	0.779 920
0.848 527	0.848 578	0.848 618
0.872 964	0.872 655	0.872 677
0.883 820	0.883 818	0.883 830

[a] $N_c = N_c' = 6$.
[b] Reference [41].
[c] Reference [42].

ones. Those are all based upon techniques that use variational wave functions for both the ground state and the intermediate states that involve large basis sets, ranging from 100 basis functions [22] to 900 [27]. Their wave functions do not include the logarithmic contributions, which can explain the large number of basis functions needed to achieve good convergence. Three of them [22,23,27] used extended (or quadruple) numerical precision to avoid round-off error propagation. Nevertheless, our calculation using basis functions that include logarithmic terms needs fewer basis functions: namely, 60 terms in the expansions given by Eqs. (13) and (14), whereas in the calculation using only one optimized β_i^μ parameter, 16 terms ($M_i = 16$) have been used in these expansions. We reiterate that we have not pushed our variationally stable approach using a coupled adiabatic hyperspherical basis to obtain the seven or more digits of accuracy necessary to achieve benchmark predictions for the static polarizabilities. To do that we would have to couple more than the 12–15 channels of each symmetry that we currently include and, in particular, we would have to include one or more of the next complete groups of channels of each symmetry. What we have shown is that for a given number of channels the inclusion of logarithmic terms allows one to obtain comparable accuracy to calculations that optimize the β parameters but do not use logarithmic terms. A key additional point is that the five digits of accuracy we have achieved at the level of approximation permitted by our computational constraints is sufficient to obtain competitive predictions for the dynamical polarizabilties, which we discuss next.

B. Dynamic polarizability

Our results for the static polarizability have determined the set of optimized parameters which provide results comparable to the use of logarithm terms in the initial- and intermediate-state expansions. We use this information to select the parameters for our calculations of the frequency-dependent (or dynamic) polarizability of He. For the dynamic case, the determined optimal values of β_i^μ for each coupled channel in the static limit have been used. We have used an equal number of coupled channels for both ground and intermediate states, that is, $N_c = N_c' = 6$ since this number of coupled channels constitutes a closed group of channels for both ground and intermediate states, according to Table IV. In Table VI, our results for the dynamic polarizability of helium are compared with previous calculations in the literature [16–19] and also with experimental values (as listed in Ref. [18]). Most calculations are unable to achieve results over the photon energy range $0.75 < \omega < 0.9$ (in a.u.) owing to the approach of the resonance region. Our calculation for the dynamic polarizability is presented in Figs. 3 and 4. In Fig. 3 one sees the rate of convergence as the number of coupled channels (with $N_c = N_c'$) increases. Figure 4 shows a comparison of our best result ($N_c = N_c' = 6$) with the theoretical results of Chung [16], Glover and Weinhold [17], and Bishop and Lam [19] as well as with experimental values from Ref. [18]. For photon frequencies $\omega < 0.7$ a.u. [Fig. 4(a)] our results compare very well with the results of other authors. However, in the resonance region [Fig. 4(b)] our calculation compares best with the results from Glover and Weinhold [17].

The resonances (sharp antisymmetric peaks) in the dynamic polarizability correspond to one-photon transitions to intermediate $^1P^o$ excited states of He. When ω approaches this region ($\omega \gtrsim 0.7$ a.u.), conventional methods start to fail due to the approximation of the poles present in Eq. (1), making the calculation increasingly difficult. As our formalism transforms Eq. (1) into Eq. (2), in which the poles have been removed, there is no difficulty in the calculation in the region $\omega > 0.7$ a.u. From the calculation of the dynamic polarizability in the resonance region, one can extract the frequencies for the one-photon transitions by simply inspecting the calculated data and, in the vicinity of an abrupt change of sign, extrapolate the values of the resonant frequencies. The first few one-photon transition energies obtained are listed in Table VII. In this table, a comparison with results of a variational calculation [41] is given. Also listed are the hyperspherical results from Ref. [42]. Unlike the usual methods for obtaining polarizabilities, one notes that the present variationally stable approach provides very accurate values for the one-photon transition energies.

V. CONCLUSIONS

In summary, we have presented a calculation for the static dipole polarizability of the helium ground state that includes logarithmic terms in both ground and intermediate states within a variationally stable, coupled-channel adiabatic hyperspherical approach. Within this basis set, the inclusion of logarithmic terms appears to be necessary to obtain convergence to the correct value of the static polarizability when nonoptimized parameters in the intermediate basis functions are used. We have shown that for any fixed number of coupled channels this approach is capable of obtaining a value for the static polarizability that is comparable to the results obtained with optimized parameters. The two methods appear comparable in their use of computer resources. Use of logarithmic terms requires more basis functions, but one does the calculation only once; use of optimized parameters—without logarithmic terms—implies fewer basis functions, but the calculations must be repeated as often as necessary to obtain the optimum values of the parameters.

Results for the dynamic polarizability have also been presented whose accuracy is comparable to that of the best results of other authors, especially in the photon frequency

range corresponding to the one-photon transitions. In fact, one of the advantages of the present approach is the ability to furnish reliable and converged results even in the resonance region due to the nonexistence of poles in the transition matrix element. These accurate predictions for the dynamical polarizability imply that our approach is capable of predicting highly accurate values for multiphoton cross sections of helium (as well as other two-electron systems). Calculations for the helium two-photon ionization cross section are in progress.

ACKNOWLEDGMENTS

We thank G.W.F. Drake for valuable discussions and for a critical reading of an early draft of this paper. This work was supported in part by the U.S. Department of Energy, Office of Science, Division of Chemical Sciences, Geosciences, and Biosciences, under Grant No. DE-FG03-96ER14646. M.M. received financial support from Fundação de Amparo à Pesquisa do Estado de São Paulo (FAPESP)-Brazil, under Grant No. 99/11363-8.

[1] J.H. Bartlett, Phys. Rev. **51**, 661 (1937).
[2] V.A. Fock, Izv. Akad. Nauk SSSR, Ser. Fiz. **18**, 161 (1954) [K. Nor. Vidensk. Selsk. Forh. **31**, 138 (1958); **31**, 145 (1958)].
[3] A.M. Ermolaev and G.B. Sochilin, Dokl. Akad. Nauk SSSR, **155**, 1050 (1964) [Sov. Phys. Dokl. **9**, 292 (1964)].
[4] K. Frankowski and C.L. Pekeris, Phys. Rev. **146**, 46 (1966).
[5] D.E. Freund, B.D. Huxtable, and J.D. Morgan III, Phys. Rev. A **29**, R980 (1984).
[6] J.D. Baker, D.E. Freund, R.N. Hill, and J.D. Morgan III, Phys. Rev. A **41**, 1247 (1990).
[7] H. Kleindienst and R. Emrich, Int. J. Quantum Chem. **37**, 257 (1990).
[8] A.J. Thakkar and T. Koga, Phys. Rev. A **50**, 854 (1994).
[9] G.W.F. Drake and Z.-C. Yan, Chem. Phys. Lett. **229**, 486 (1994).
[10] S.P. Goldman, Phys. Rev. A **57**, R677 (1998).
[11] G.W.F. Drake, Phys. Scr. **T83**, 83 (1999).
[12] G.W.F. Drake, M.M. Cassar, and R.A. Nistor, Phys. Rev. A **65**, 054501 (2002).
[13] V.I. Korobov, Phys. Rev. A **61**, 064503 (2000).
[14] V.I. Korobov, Phys. Rev. A **66**, 024501 (2002).
[15] Yu.V. Popov and L.U. Ancarani, Phys. Rev. A **62**, 042702 (2000).
[16] K.T. Chung, Phys. Rev. **166**, 1 (1968).
[17] R.M. Glover and F. Weinhold, J. Chem. Phys. **65**, 4913 (1976).
[18] E.-A. Reinsch, J. Chem. Phys. **83**, 5784 (1985), Table I.
[19] D.M. Bishop and B. Lam, Phys. Rev. A **37**, 464 (1988).
[20] B. Gao, C. Pan, C.R. Liu, and A.F. Starace, J. Opt. Soc. Am. B **7**, 622 (1990).
[21] H.P. Saha and C.D. Caldwell, Phys. Rev. A **44**, 5642 (1991).
[22] D.M. Bishop and J. Pipin, Int. J. Quantum Chem. **45**, 349 (1993).
[23] A.K. Bhatia and R.J. Drachman, J. Phys. B **27**, 1299 (1994).
[24] M.J. Jamieson, G.W.F. Drake, and A. Dalgarno, Phys. Rev. A **51**, 3358 (1995).
[25] Z.-C. Yan, J.F. Babb, A. Dalgarno, and G.W.F. Drake, Phys. Rev. A **54**, 2824 (1996).
[26] S.J.A. van Gisbergen, F. Kootstra, P.R.T. Schipper, O.V. Gritsenko, J.G. Snijders, and E.J. Baerends, Phys. Rev. A **57**, 2556 (1998).
[27] K. Pachucki and J. Sapirstein, Phys. Rev. A **63**, 012504 (2000).
[28] K.D. Bonin and M.A. Kadar-Kallen, Int. J. Mod. Phys. B **8**, 3313 (1994).
[29] B. Gao and A.F. Starace, Phys. Rev. Lett. **61**, 404 (1988).
[30] B. Gao and A.F. Starace, Phys. Rev. A **39**, 4550 (1989).
[31] C.R. Liu, B. Gao, and A.F. Starace, Phys. Rev. A **46**, 5985 (1992).
[32] M. Masili and A.F. Starace, Phys. Rev. A **62**, 033403 (2000).
[33] U. Fano, Rep. Prog. Phys. **46**, 97 (1983).
[34] J.M. Feagin, J.H. Macek, and A.F. Starace, Phys. Rev. A **32**, 3219 (1985).
[35] J.E. Hornos, S.W. MacDowell, and C.D. Caldwell, Phys. Rev. A **33**, 2212 (1986); **34**, 2535 (1986).
[36] M. Masili, J.E. Hornos, and J.J. De Groote, Phys. Rev. A **52**, 3362 (1995).
[37] C.D. Lin, Phys. Rep. **257**, 1 (1995), and references therein.
[38] J.H. Macek, J. Phys. B **1**, 831 (1968).
[39] A.F. Starace and G.L. Webster, Phys. Rev. A **19**, 1629 (1979).
[40] H.T. Coelho and J.E. Hornos, Phys. Rev. A **43**, 6379 (1991).
[41] A. Kono and S. Hattori, Phys. Rev. A **34**, 1727 (1986).
[42] M. Masili, J.J. De Groote, and J.E. Hornos, J. Phys. B **33**, 2641 (2000).
[43] B. Schiff, H. Lifson, C.L. Pekeris, and P. Rabinowitz, Phys. Rev. **160**, A1104 (1965).
[44] C.R. Mansfield and E.R. Peck, J. Opt. Soc. Am. **59**, 199 (1969).
[45] P.W. Langhoff and M. Karplus, J. Opt. Soc. Am. **59**, 863 (1969).
[46] D. Gugan and G.W. Michel, Mol. Phys. **39**, 783 (1980).
[47] D. Gugan, Metrologia **28**, 405 (1991).
[48] K. Grohmann and H. Luther, *Temperature—Its Measurement and Control in Science and Industry* (AIP, New York, 1992), Vol. 6, p. 21.